J|A|C|S
ARTICLES
Published on Web 05/12/2006

Proton Transfer-Induced Conformational Changes and Melting In Designed Peptides in the Gas Phase

Motoya Kohtani, Thaddeus C. Jones, Rajagopalan Sudha, and Martin F. Jarrold*

Contribution from the Department of Chemistry, Indiana University, 800 East Kirkwood Avenue, Bloomington, Indiana 47405

Received October 2, 2005; E-mail: mfj@indiana.edu

Abstract: The conformations of protonated $RA_{15}K$, $RA_{20}K$ and $RA_{15}H$ (R = arginine, A = alanine, K = lysine, and H = histidine) have been examined in the gas phase as a function of temperature. These peptides were designed so that intramolecular proton transfer will trigger conformational changes between a helix (proton sequestered at the C-terminus) and globule (proton sequestered at the N-terminus). Kinetically controlled structural transitions occur below 400 K (from helix to globule for $RA_{15}H$, and from globule to helix for $RA_{15}K$ and $RA_{20}K$). As the temperature is raised, the compact globule found at room temperature expands, accesses more configurations, and becomes entropically favored. At around 500 K, the $RA_{15}K$ and $RA_{20}K$ helices undergo a melting transition. The transition is broad, as expected for a phase transition in a finite system, and becomes narrower as the peptide size increases. In the helical conformation, the two basic residues are well separated; as a result, the proton transfer necessary to drive the melting transition probably involves a mobile proton. For doubly protonated $RA_{15}K$, a dumbbell-like conformation (resulting from repulsion between the two protonated basic residues) is found at high temperature.

Introduction

Rapid intramolecular proton transfer to give a "mobile proton" is believed to play a critical role in directing peptide fragmentation in the gas phase.[1−9] Since peptide fragmentation patterns can provide the sequence information needed in applications such as proteomics, a basic understanding of the fragmentation process, including issues such as proton mobility and the conformation of the dissociating state, is important. Here we report studies of model peptides designed so that intramolecular proton transfer triggers a conformational change. The peptides have a polyalanine core with a single basic residue at each end. Intramolecular proton transfer from one basic group to the other induces a switch between helical and globular conformations. When the proton is at the C-terminus, the helix is stabilized by favorable interactions between the charge and the helix dipole. When the proton is at the N-terminus, this interaction destabilizes the helix and a globule (a compact random-looking, three-dimensional structure) results.

The specific peptides that we report on here are protonated $RA_{15}K$, $RA_{20}K$, and $RA_{15}H$ (R = arginine, A = alanine, K = lysine, and H = histidine). We find kinetically controlled transitions between helical and globular conformations occur at close to room temperature. However, as the temperature is raised, the globular conformation expands, accesses more conformations, and becomes entropically favored. The helices then undergo a melting transition at around 500 K. The transition is broad, as expected for a phase transition in a finite system, and becomes narrower as the peptide size increases.

We use ion mobility measurements to probe the peptide conformations as a function of temperature.[10,11] The mobility of an ion (how rapidly it moves through a buffer gas under the influence of a weak electric field) depends on the ions average collision cross section with the buffer gas: ions with small compact geometries have fewer collisions and travel through the buffer gas more rapidly. Geometries are assigned by comparing the measured cross sections to average cross sections calculated for trial geometries, which are usually derived from molecular dynamics simulations.

Methods

The experimental apparatus used for these studies consists of an electrospray source interfaced to a 30.8 cm long high-temperature drift tube, followed by a quadrupole mass spectrometer. A detailed description is provided elsewhere.[12,13] Briefly, electrosprayed ions enter the

(1) Johnson, R. S.; Martin, S. A.; Biemann, K. *Int. J. Mass Spectrom. Ion Processes* **1988**, *86*, 137−154.
(2) Burlet, O.; Orkiszewski, R. S.; Ballard, K. D.; Gaskell, S. J. *Rapid Commun. Mass Spectrom.* **1992**, *6*, 658−662.
(3) McCormack, A. L.; Somogyi, A.; Dongré, A. R.; Wysocki, V. H. *Anal. Chem.* **1993**, *65*, 2859−2872.
(4) Jones, J. L.; Dongré, A. R.; Somogyi, A.; Wysocki, V. H. *J. Am. Chem. Soc.* **1994**, *116*, 8368−8369.
(5) Cox, K. A.; Gaskell, S. J.; Morris, M.; Whiting, A. *J. Am. Soc. Mass Spectrom.* **1996**, *7*, 522−531.
(6) Dongré, A. R.; Jones, J. L.; Somogyi, A.; Wysocki, V. H. *J. Am. Chem. Soc.* **1996**, *118*, 8365−8374.
(7) Nair, H.; Wysocki, V. H. *Int. J. Mass Spectrom. Ion Processes* **1998**, *174*, 95−100.
(8) Vaisar, T.; Urban, Y. *J. Mass Spectrom.* **1998**, *33*, 505−524.
(9) Wysocki, V. H.; Tsaprailis, G.; Smith, L. L.; Breci, L. A. *J. Mass Spectom.* **2000**, *35*, 1399−1406.
(10) Clemmer, D. E.; Jarrold, M. F. *J. Mass Spectrom.* **1997**, *32*, 577−592.
(11) Wyttenbach, T.; Bowers, M. T. *Top. Curr. Chem.* **2003**, *225*, 207−232.
(12) Kinnear, B. S.; Hartings, M. R.; Jarrold, M. F. *J. Am. Chem. Soc.* **2001**, *123*, 5660−5667.
(13) Kohtani, M.; Schneider, J. E.; Jones, T. C.; Jarrold, M. F. *J. Am. Chem. Soc.* **2004**, *126*, 16981−16987.

apparatus through a heated capillary interface maintained at 135−145 °C and pass through a differentially pumped region before being focused into the drift tube. The drift tube contains helium buffer gas at 3−5 Torr. Ions travel through the drift tube under the influence of a uniform electric field of 5−13 V cm^{-1}. The temperature of the drift tube can be adjusted from room temperature up to 1100 K. After traveling across the drift tube, some of the ions exit through a small aperture. The ions that exit are focused into a quadrupole mass spectrometer, where they are mass analyzed and then detected. An electrostatic shutter at the entrance of the drift tube can be pulsed to permit short (100 μs) packets of ions to enter the drift tube. The arrival time distribution of the ions at the detector is recorded using a multichannel scaler synchronized with the ion shutter. Drift times are determined from the arrival time distributions and converted into collision cross sections using standard methods.[14]

To calculate cross sections for comparison with the experimental results, trial geometries were obtained from molecular dynamics simulations. The molecular dynamics simulations were performed with the MACSIMUS suite of programs[15] using the CHARMM 21.3 parameter set. Average collision cross sections were calculated for trial geometries (see below) by the trajectory method using MOBCAL.[16,17] In MOBCAL, the long range interactions between the ion and buffer gas (helium in this case) are treated using empirical potentials. The trajectory method correctly accounts for multiple scattering events between a buffer gas atom and the ion.

The peptides were synthesized using *FastMoc* chemistry on an Applied Biosystems 433A peptide synthesizer. After synthesis, they were cleaved from the HMP resin using a 90% trifluoroacetic acid (TFA), 5% thioanisole, 3% ethanediol, and 2% anisole cocktail, precipitated using cold diethyl ether, and lyophilized. The peptides were used without further purification. Electrospray solutions were prepared by dissolving 1 mg of peptide in 1 mL of TFA and 0.1 mL of purified water and electrosprayed directly. All of the peptides studied here were acetylated at the N-terminus prior to deprotection of the basic side chains. Dimers and higher-order multimers, which can be identified from their mobilities, were not abundant under the conditions used for these studies.

Results and Discussion

Figure 1 shows drift time distributions and cross sections recorded for protonated $RA_{15}K$. At close to room temperature the drift time distributions show two peaks, indicating the presence of two conformations which can be assigned to a helix (longer drift time) and globule (shorter drift time) on the basis of cross sections calculated for structures derived from molecular dynamics simulations (see below). Between 333 and 373 K a bridge grows between the two peaks, and then the globule peak disappears. This behavior indicates that the globule is converting into the helix as the ions travel through the drift tube.

The gas-phase basicity of the guanidine group of arginine is around 70 kJ mol^{-1} larger than the ϵ-amino group of lysine;[18] thus, in the absence of any other factor, arginine is the most favorable protonation site in the $RA_{15}K$ peptide, and it is expected to be the preferred protonation site in the globular conformation. However, when the lysine residue is protonated, the $RA_{15}K$ peptide can form a helix that is stabilized by electrostatic interactions between the charge and the helix dipole and by helix capping interactions (where the protonated amine

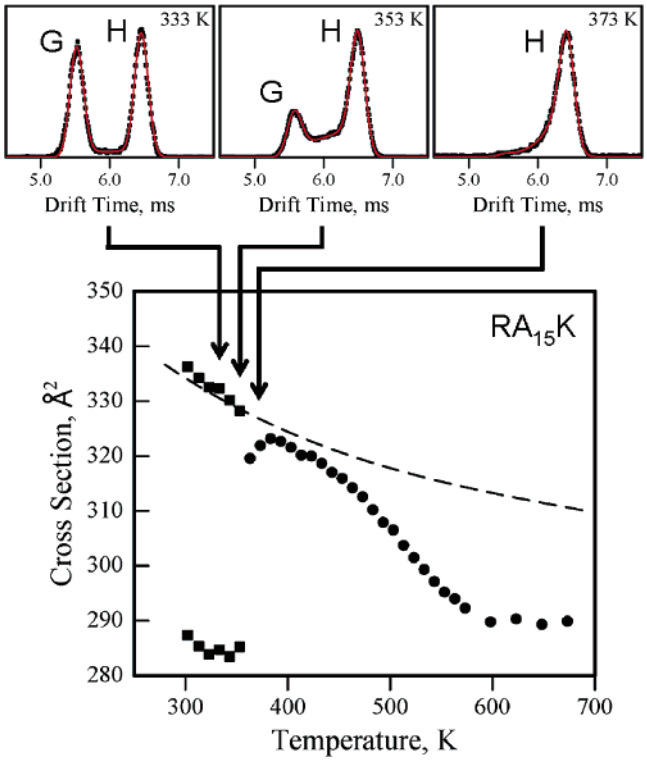

Figure 1. Drift time distributions and cross sections determined for protonated $RA_{15}K$ as a function of temperature. In the drift time distributions, the points represent the measurements, and the solid red lines that go through the points are fits to deduce rate constants for conversion of the globule into the helix. In the plot of the cross sections, the squares represent values determined from the center of the helix and globule peaks (when they are resolved), whereas the circles show cross sections obtained by averaging over the drift time distributions for the single merged peak observed at higher temperatures. The dashed line in the main figure shows the average cross sections calculated for a "frozen" helix (see text) as a function of temperature.

hydrogen bonds to the dangling carbonyl groups at the end of the helix).[19] The observation that the globule converts into the helix as the ions travel through the drift tube at 333−373 K indicates that the helix (protonated at the lysine) has a lower free energy than the globule (protonated at the arginine) at close to room temperature. Thus, the extra stabilizing interactions that are present for the helix must more than compensate for the difference in gas-phase basicity between lysine and arginine. Since the helix has a lower free energy than the globule, the globule that is present at room temperature must be trapped in a metastable state. The metastable globule converts into a helix when heated to the point where the rate constants become large enough to drive the conversion on the experimental time scale.

In the temperature range where conversion between the globule and helix occurs on a time scale comparable to the drift time, the drift time distributions can be fit to obtain the rate constant for the globule-to-helix transition.[12,20] The solid red line that goes through the points in the drift time distributions in Figure 1 is the result of such a fit. Rate constants determined in this way provide a linear Arrhenius plot ($R^2 = 0.99$) with $E_a = 85 \pm 2$ kJ mol^{-1} and $\log A = 14.8 \pm 0.2$. Similar results were obtained for $RA_{20}K$ with $E_a = 75 \pm 2$ kJ mol^{-1} and $\log A = 13.2 \pm 0.2$. Isomerization from the globule to the helix

(14) Mason, E. A.; McDaniel, E. W. *Transport Properties of Ions in Gases*; Wiley: New York, 1988.
(15) http://www.icpf.cas.cz/jiri/macsimus/default.htm.
(16) Mesleh, M. F.; Hunter, J. M.; Shvartsburg, A. A.; Schatz, G. C.; Jarrold M. F. *J. Phys. Chem.* **1996**, *100*, 16082−16086.
(17) http://nano.chem.indiana.edu/software.html.
(18) NIST Chemistry WebBook: http://webbook.nist.gov/chemistry/.
(19) Hudgins, R. R.; Ratner, M. A.; Jarrold, M. F. *J. Am. Chem. Soc.* **1998**, *120*, 12974−12975.
(20) Gatland, I. R. *Case Stud. At. Phys.* **1974**, *4*, 369−437.

must involve proton transfer from the more basic arginine at the N-terminus to the less basic lysine at the C-terminus, because protonation at the C-terminus is required to stabilize the helical conformation. As noted above, the difference between the intrinsic gas-phase basicities of the lysine and arginine side chains is around 70 kJ mol^{-1} which is only slightly less than the measured activation energies. In an effort to determine whether proton transfer is the rate-limiting step in these reactions, we measured rate constants for deuterated $RA_{15}K$ obtained by electrospraying from a mixture of CF_3COOD and D_2O after a 30 min incubation period. The mass spectrum showed a distribution of 15−19 deuterium substitutions out of a maximum of 25 exchangeable hydrogens. It is surprising that full exchange is not observed under these conditions. However, $RA_{15}K$ has a hydrophobic core, and it is possible that some of the backbone amides remain protected in solution. The rate constants measured for the deuterated peptides are almost identical to those measured with the natural isotope abundance, so there does not appear to be a significant kinetic isotope effect. This suggests that proton/deuteron transfer from the arginine to the lysine is not the rate-limiting step in the conversion of the globule into the helix, and so the rate-limiting step is presumably the conformational changes that either precede or follow proton transfer. In view of the fact that full exchange is not observed for $RA_{15}K$, we should mention that there remains a possibility that the transferred species is still an H^+. However, while it is feasible that H^+ transfer occurs in some of the deuterated peptides, it is difficult to imagine that it occurs in the majority.

For temperatures above about 400 K a single merged peak is observed in the drift time distributions (see Figure 1). Above about 450 K the peak width becomes diffusion limited (i.e. the measured peak shape becomes identical to that calculated for a single conformation in the diffusion limit). This indicates that all the ions have virtually identical mobilities, which could result from either a single conformation, a narrow range of conformations with almost identical mobilities, or rapid conformational averaging as the ions travel through the drift tube.

The dashed line in Figure 1 shows the average cross sections calculated for a "frozen" helix as a function of temperature. The "frozen" helix is a single snapshot taken from the lowest energy of ten 360 ps, room-temperature molecular dynamics simulations initiated from an α-helical conformation. The cross sections calculated for this structure as a function of temperature show how the cross sections should change if the structure remains fixed (or frozen) as the temperature is raised. Deviations of the measured cross sections from this behavior indicate a conformational change. The calculated average collision cross sections for the "frozen" helix decrease as the temperature increases. This decrease in the cross sections occurs because the long-range interactions between the ion and buffer gas become less important, and the collisions become harder, as the temperature is raised. It is evident that above a temperature of about 440 K the measured cross sections fall further and further from the behavior expected for the "frozen" helix. This indicates that a conformational change is occurring. At around 580 K, the cross sections level off at a value that is quite close to the room-temperature cross sections for the compact globule and then remain constant up to around 673 K, at which point the peptide is almost entirely dissociated. The main fragments

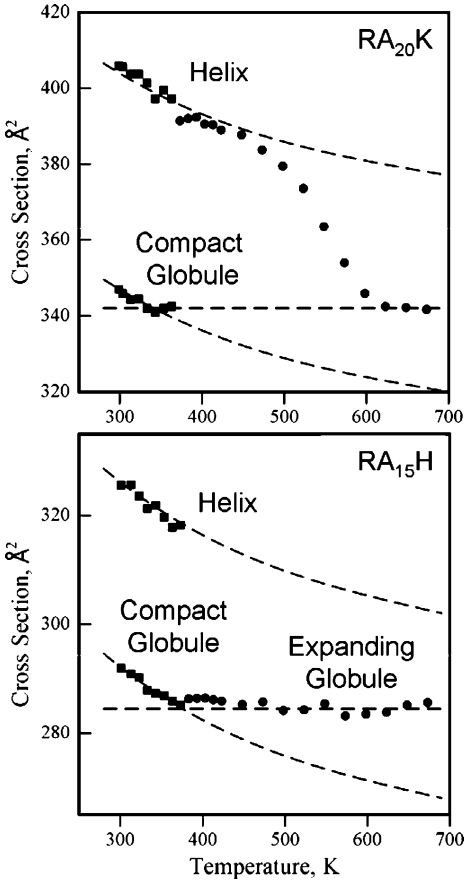

Figure 2. Cross sections measured for protonated $RA_{20}K$ and $RA_{15}H$ as a function of temperature. The squares represent values determined from the center of the helix and globule peaks observed at lower temperatures. The circles show cross sections obtained by averaging over the drift time distributions for the single merged peak observed at higher temperatures. The dashed lines that decrease with increasing temperature show the calculated cross sections for a "frozen" helix (upper) and "frozen" globule (lower). The horizontal dashed lines are guides that show the expected position for the expanding globule (see text).

are the b_n^+, b_{n-1}^+, b_{n-2}^+, etc. series using standard notation.[21] The high mass b ions are most abundant, and the intensities systematically fall with decreasing mass. This series of fragment ions is consistent with the proton being located on the N-terminus arginine.

Figure 2 shows cross sections measured for $RA_{20}K$ and $RA_{15}H$. The results for $RA_{20}K$ are similar to those for $RA_{15}K$: both the helix and compact globule exist at room temperature; as the temperature is raised, the globule converts into the helix, and the cross sections then drop and level-off at close to the room-temperature value for the compact globule. For $RA_{15}H$ both the helix and globule are observed at low temperature, but as the temperature is raised, the helix converts into the globule. The gas-phase basicity of the imidizole side chain of histidine is expected to be around 20 kJ mol^{-1} larger than that of the ϵ-amino group of lysine (based on a comparison of the gas-phase basicity of butylamine and imidizole). Thus, for the globule to be the lowest-energy conformation for $RA_{15}H$, the protonated imidizole side chain of histidine must be considerably less effective at stabilizing the helix than the protonated amino group of lysine. The origin of the lower helix stabilizing capability of histidine is almost certainly a steric effect: the

(21) Bieman, K. *Methods Enzymol.* **1990**, *193*, 886−887.

charge is distributed between two widely spaced NH groups in the protonated side chain of histidine, and only one of these groups (at a time) can hydrogen bond with the dangling CO groups at the end of the helix, leaving the other unshielded. All three hydrogens in the protonated amino group of lysine can simultaneously hydrogen bond to the dangling CO groups at the end of the helix. Thus, histidine is less effective at stabilizing a helix than lysine.

The dashed lines that go through the low temperature points for the $RA_{20}K$ and $RA_{15}H$ globules in Figure 2 show the calculated cross sections for "frozen" globules. Here we have taken snapshots from the lowest-energy room-temperature molecular dynamics simulation for the globules and calculated the average cross sections for these structures as a function of temperature. The results show the expected temperature dependence for globules that retain the same geometry as the temperature is raised. As with the "frozen" helix considered above, the cross sections for the "frozen" globules systematically decrease with increasing temperature. A deviation from this predicted behavior indicates a conformational change. Above about 380 K, the measured cross sections for $RA_{15}H$ stop tracking the dashed line for the "frozen" globule and subsequently change little as the temperature is raised further. This behavior suggests that the globule starts to expand above 380 K. At room temperature, the compact globule is essentially close packed. The close packing severely restricts the number of conformations that are accessible to the compact globule so that this conformation is not entropically favored with respect to the helix.[22] Indeed, finding low-energy compact globular conformations by molecular dynamics and Monte Carlo methods is exceedingly difficult because there are so few of them.[23] The expansion of the globule allows it to access more conformations so that it becomes more entropically favored as the temperature is raised. In the high-temperature limit where the strength of the intramolecular interactions that hold the globule together are small compared to thermal energy, the expanding globule will become a random coil. However, it appears that the peptides dissociate before reaching this limit.

For both $RA_{15}K$ and $RA_{20}K$, a single narrow peak moves from a position close to that expected for the helix to one close to that expected for the expanding globule as the temperature is raised from around 450 to 600 K. This behavior suggests that there is rapid interconversion between the helix and globule and that the population is shifting from being predominantly helical at around 450 K to predominantly expanded globule at around 600 K. Under these circumstances the position of the peak reflects the amount of time spent in each conformation, and it can be used to derive an equilibrium constant when the positions of the two interconverting forms can be identified (as they are in the figure by the dashed lines for the helix and expanding globule). Figure 3 shows a plot of ln K against $1/T$ for equilibrium constants determined in this way for $RA_{20}K$. From this plot we can deduce $\Delta H^\circ = 97 \pm 17$ kJ mol^{-1} and $\Delta S^\circ = 178 \pm 35$ JK^{-1}mol^{-1}. A similar analysis for $RA_{15}K$ yields $\Delta H^\circ = 60 \pm 10$ kJ mol^{-1} and $\Delta S^\circ = 116 \pm 23$ JK^{-1}mol^{-1}. The entropy changes are relatively large and must be primarily due to the change in the backbone configurational entropy on going from the helix to the expanded globule.

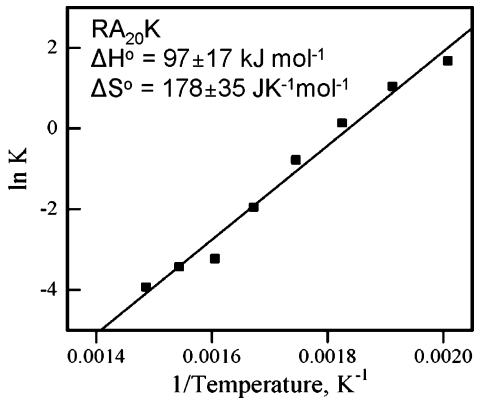

Figure 3. Plot of ln K against $1/T$ for equilibrium constants determined for $RA_{20}K$.

Table 1. Comparison of Enthalpy and Entropy Changes Measured for Helix Melting Transitions for Protonated $RA_{15}K$ and $RA_{20}K$ (this work) with Those Calculated for neutral A_{15} and A_{20} (from ref 25)

peptide	ΔH, kJ mol^{-1}	ΔS, J K^{-1} mol^{-1}
A_{15}	56	105
$RA_{15}K$	60	116
A_{20}	123	233
$RA_{20}K$	97	178

The transition from helix to expanded globule that occurs for $RA_{15}K$ and $RA_{20}K$ at around 500 K is driven by entropy and occurs with a concomitant increase in the enthalpy. The resulting step in the enthalpy will cause a peak in the heat capacity; in other words there is a latent heat associated with this transition. So the transition has many of the characteristics of a finite size analogue of a first-order phase transition. As expected for a finite system, the melting transition is broad. However, note that the transition for $RA_{20}K$ is significantly sharper than for $RA_{15}K$, a sharpening of the transition with increasing size is another characteristic of phase transitions in finite systems. Recent simulations suggest that helix−coil transitions occur for neutral, unsolvated polyalanine peptides.[24−26] The transitions, which take place at around 500 K, are first order (they occur with a latent heat). Although the authors refer to these as helix−coil transitions, it is likely that the coil state is not completely random, and residual intramolecular interactions make it quite similar to our expanded globule identified here. The calculated enthalpy and entropy changes associated with the helix−coil transitions for A_{15} and A_{20} are compared in Table 1 to the enthalpy and entropy changes deduced for $RA_{15}K$ and $RA_{20}K$ from the equilibrium constants. The calculated enthalpy and entropy changes are quite similar to the measured values.

The high-temperature behavior reported here for $RA_{15}K$ is quite different from that previously found for protonated $A_{15}K$.[27] For this peptide the helix is the only conformation observed at low temperature, and the helical conformation persists up to 750 K where $A_{15}K$ is almost entirely dissociated. $RA_{15}K$ on

(22) Kinnear, B. S.; Hartings, M. R.; Jarrold, M. F. *J. Am. Chem. Soc.* **2002**, *124*, 4422−4431.
(23) Damsbo, M.; Kinnear, B. S.; Hartings, M. R.; Ruhoff, P. T.; Jarrold, M. F.; Ratner, M. A. *Proc. Natl. Acad. Sci. U.S.A.* **2004**, *101*, 7215−7222.
(24) Okamoto, Y.; Hansmann, U. H. E. *J. Phys. Chem.* **1995**, *99*, 11276−11287.
(25) Alves, N. A.; Hansmann, U. H. E. *Phys. Rev. Lett.* **2000**, *84*, 1836−1839.
(26) Peng, Y.; Hansmann, U. H. E.; Alves, N. A. *J. Chem. Phys.* **2003**, *118*, 2374−2380.
(27) Kohtani, M.; Jones, T. C.; Schneider, J. E.; Jarrold, M. F. *J. Am. Chem. Soc.* **2004**, *126*, 7420−7421.

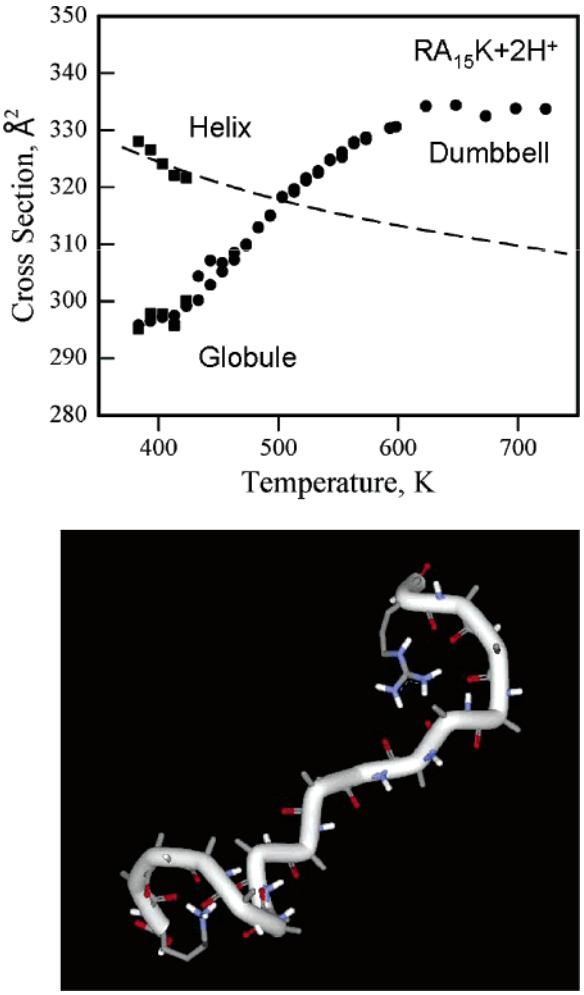

Figure 4. (Top) Cross sections measured for doubly protonated $RA_{15}K$ as a function of temperature. (■) Values determined from the center of the helix and globule peaks observed at lower temperatures. (●) Cross sections obtained by averaging over the drift time distributions for the single merged peak observed at higher temperatures. (Bottom) Dumbbell structure found in molecular dynamics simulations for $RA_{15}K$ protonated at both basic residues at high temperature.

the other hand starts converting into a globule at 450 K, a temperature where $A_{15}K$ is solidly helical. How does the proton know to move to the N-terminus of $RA_{15}K$ while apparently remaining locked at the C-terminus of $A_{15}K$? This conundrum can be explained by a partially mobile proton. We suggest that as the temperature is raised the proton has a small but finite probability of detaching from the lysine side chain and rapidly transferring between backbone carbonyl and amide groups, before becoming relocalized at a basic residue (the same or a different one). For $A_{15}K$, there is only one basic site (the N-terminus is acetylated) so the proton must relocalize at the C-terminus lysine; as a result, this peptide remains helical.

In $RA_{15}K$ and $RA_{20}K$, the proton presumably makes its way to the N-terminus where it is trapped by the arginine. Once the proton is sequestered by the arginine, it disrupts the helix and drives the peptide into a globular conformation. According to this interpretation, the proton must become partially mobile (on the time scale of the experiments) at below 450 K.

In the preceding studies we investigated singly protonated $RA_{15}K$, $RA_{20}K$, and $RA_{15}H$. Electrospray also generates doubly protonated ions. Figure 4 shows cross sections measured for doubly protonated $RA_{15}K$. At room temperature two peaks are observed in the drift time distributions that can be attributed to helical and globular conformations. As the temperature is raised, the helix disappears, converting into the globule. The location of the second charge in the doubly protonated $RA_{15}K$ helix is an interesting issue. In previous studies of doubly protonated A_nK peptides, simulations suggested that the preferred location of the second proton was an amide CO near the C-terminus. The helix was disrupted if the second proton was located near the middle of the peptide or near the N-terminus. When both protons are near the C-terminus, favorable interactions with the helix dipole must compensate for their mutual repulsion. At temperatures above 400 K the cross sections for the globule increase (see Figure 4) and level-off at a value significantly above those expected for the helix. In molecular dynamics simulations, $RA_{15}K$ protonated at both basic residues adopts a dumbbell-like structure at high temperature, where each protonation site is surrounded by a small self-solvation shell; an example is shown in the lower half of Figure 4. Since the doubly charged ion remains compact at low temperatures, the unfolding that occurs as the temperature is raised cannot result from Coulombic repulsion alone. It must result from a combination of Coulombic repulsion and entropic effects (the unfolded structure has a higher entropy than the globule). The entropic effects alone, however, are not enough to unfold the singly charged ions to the same extent.

Conclusions

The $RA_{15}K$, $RA_{20}K$, and $RA_{15}H$ peptides studied here were designed so that intramolecular proton transfer triggers a conformational change between a helix and globule. Kinetically controlled structural transitions occur at close to room temperature, but as the temperature is raised, the globular conformation expands, accesses more conformations, and becomes entropically favored. The helices then melt at around 500 K. The melting transition is broad, as expected for a phase transition in a finite system, and becomes narrower as the peptide size increases. The measured entropy and enthalpy changes for helix melting are quite similar to values calculated for neutral A_{15} and A_{20} peptides.

Acknowledgment. We thank the National Institutes of Health for support.

JA056745S